JOURNAL OF Applied Polymer SCIENCE

Thermal, Electrical, and Mechanical Properties of Polyethylene–Graphene Nanocomposites Obtained by *In situ* Polymerization

Fabiana de C. Fim,[1] Nara R. S. Basso,[2] Ana P. Graebin,[2] Denise S. Azambuja,[1] Griselda B. Galland[1]
[1]Universidade Federal do Rio Grande do Sul, Avenida Bento Gonçalves, 9500, Porto Alegre 91570-970, Brazil
[2]Pontifícia Universidade Católica do Rio Grande do Sul-Brasil, Avenida Ipiranga 6681, Porto Alegre 90619-900, Brazil
Correspondence to: G. B. Galland (E-mail: griselda.barrera@ufrgs.br)

ABSTRACT: In this study, we investigated the thermal, dynamic mechanical, mechanical, and electrical properties of polyethylene (PE)–graphene nanosheet (GNS) nanocomposites, with GNS amounts from 0 to 20 wt %, prepared by *in situ* polymerization. The thermal stability was evaluated by thermogravimetric analysis (TGA) and showed that the addition of GNSs to the polyolefin matrix increased the onset degradation temperature by 30°C. The electrical conductivity, measured by the impedance technique, presented a critical percolation threshold of 3.8 vol % (8.4 wt %) of GNS. A slight decrease in the tensile strength was found. On the other hand, dynamic mechanical analysis showed an increase in the storage modulus of the nanocomposites compared with that of neat PE. The glass-transition temperature value increased from −111°C (neat PE) to −106°C (PE/6.6 wt % GNS). All of these results show that PE became stiffer and thermally more stable and could be transformed from an insulator to a semiconductor material in the presence of GNSs. © 2012 Wiley Periodicals, Inc. J. Appl. Polym. Sci. 000: 000–000, 2012

KEYWORDS: catalysts; polyolefins; graphene and fullerenes; mechanical properties; nanotubes; thermal properties

Received 7 May 2012; accepted 7 July 2012; published online
DOI: 10.1002/app.38317

INTRODUCTION

Polyethylene (PE) is one of the main polymers produced in the world because of its low cost, recyclability, easy processing, and versatility. Among PEs, high-density polyethylene (HDPE) stands out for its high tensile strength, which results from its crystalline structure, high molecular weight, and low branch content. On the other hand, HDPE has properties that could be improved, such as its gas barrier properties, thermal stability, and electrical conductivity, to broaden its applications. The improvement of these properties could be achieved with the addition of fillers to the PE matrix.[1]

In recent years, research on polymer nanocomposites has advanced significantly because of their high potential as materials with novel properties.[2] The incorporation of nanofillers in the polymeric matrix yields specific properties and a wide range of applications.[3] Recent studies in nanocomposites have involved fillers such as clays,[4,5] carbon nanotubes,[6] carbon nanofibers,[7] silica,[8] and graphite.[9]

Graphite is chemically similar to carbon nanotubes and structurally analogous to layered silicate or clays. Graphite is composed by graphene layers, which include single-layer graphene, the strongest material ever measured, with a Young's modulus of 1 TPa and an ultimate strength of 130 GPa.[10] Hence, graphite is a nanofiller with the potential to improve the properties of neat polymers.[11] Graphite and PE are commodity materials that offer significant economic advantages over carbon nanotubes, fillers that have been studied more in nanocomposite formulations.[12] Graphite has been used as natural graphite flakes,[13] oxidized,[14] expanded, and as graphene nanosheets (GNS).[15] GNSs are obtained when the exfoliated graphite is ultrasonicated and has the advantage of having nanometric dimensions, which qualifies this material to be used in obtaining nanocomposites.

Wong et al.[13] prepared HDPE composites by melt processing with a compounder, using two different kinds of graphite: untreated and expanded graphite. The electrical and mechanical properties of the composites were evaluated and compared. The composite with expanded graphite showed an improvement in electrical conductivity and stiffness compared to the original HDPE.

Some properties, such as the mechanical properties, depend on good dispersion of the filler in the polymeric matrix. Thus, many authors have used a coupling agent to obtain good dispersion of graphite in PE. High-speed mixed nanocomposites of graphite and HDPE were prepared by Wang and Chen[16] with a

surfactant to prevent aggregation of the GNSs. They obtained an increase of 290% in the elongation at break with 10 wt % modified filler. In a recent work,[17] researchers used vinyl triethoxysilane as a coupling agent to obtain low-density polyethylene (LDPE)–graphene nanocomposites by solution in toluene. The reinforcement of graphene resulted in increases of up to 27.0 and 92.8% in the tensile strength and Young's modulus values, respectively, of the nanocomposites compared to those of neat LDPE. Recently, Macosko et al.[18] compared the properties of linear low-density polyethylene (LLDPE)–GNS nanocomposites obtained via solvent blending and melt compounding using neat and functionalized LLDPE with amino and cyano groups. They concluded that the GNSs dispersed better in functionalized LLDPE via solvent blending, and this enhanced the mechanical properties. However, the electrical conductivity was more pronounced for nanocomposites obtained with unfunctionalized PE.

The electrical properties are enhanced when the filler is more agglomerated. Segregated network composites materials have been found to have a lower percolation threshold compared with composites with randomly distributed conductive fillers.[12(a)] The percolation threshold of HDPE–GNS obtained by conventional extrusion and injection-molding methods is normally 10–15 vol %. Jiang and Drzal[19] reduced the percolation threshold to 3–5 vol % using processing techniques that induced the selective aggregation of GNSs at the HDPE–GNS interface; on the other hand, the mechanical properties were reduced. A GNS/ultra-high-molecular-weight PE composite with a segregated structure was fabricated with a water–ethanol solvent-assisted dispersion and hot compression at 200°C. A percolation threshold as low as 0.07 vol % was achieved with the formation of a two-dimensional conductive network.[20]

All the works already published that prepared graphite–PE nanocomposites have used fusion or a mixture of the polymer with the nanofiller. *In situ* polymerization, where the polymer grows in the presence of the nanofiller, appears to be an attractive route for obtaining well-dispersed PE–graphene nanocomposites. Effectively, in a recent study,[21] we prepared PE–GNS nanocomposites by this method. The purpose of this study was to examine the properties of the nanocomposites described in the previous work because there seem to be no reports on the behavior of PE–GNS nanocomposites obtained by *in situ* polymerization.

EXPERIMENTAL

Preparation of PE–Graphene Nanocomposites

The expanded graphite (Micrograf HC11 from Nacional Grafite, Ltda., Minas Gerais, Brazil) was suspended in 70% ethanol, and the suspension was treated with an ultrasound bath for 8 h to obtain the GNSs. The GNSs were stirred with 15 wt % methylaluminoxane for 30 min in toluene. The solvent was then eliminated under reduced pressure. The treated GNSs were added to the reactor as filler in variable amounts. The polymerization reactions were carried in a 100-mL PARR reactor. Toluene was used as the solvent, methylaluminoxane was used as the cocatalyst (Al/Zr = 1000), and Cp_2ZrCl_2 was used as the catalyst (2×10^{-6} mol). The reactions were done at 70°C with an ethylene pressure of 2.8 bar for 30 min.[21] The amount of GNSs in the nanocomposites is also given in volume percentage to compare it with those in other works. The percentage in volume was calculated from the percentage in weight and the GNS (2.25 g/cm^3) and PE (0.96 g/cm^3) densities, respectively.

Thermal Analysis

The nanocomposite thermal stability was determined by thermogravimetric analysis (TGA) with a Universal V2.6D analyzer (TA Instruments, New Castle/USA) at a heating rate of 20°C/min. The samples (from 10 to 15 mg) were heated from 25 to 1000°C in an inert atmosphere (nitrogen).

Tensile Testing

The tensile strength and modulus were determined according to the ASTM D 638 type V with a universal testing machine (model EMIC DL 10000, EMIC, Paraná/Brazil) at a crosshead speed of 30 mm/min at room temperature. The nanocomposites were injection-molded at 165°C with a pressure of 250 bar for 4 s in a Haake mini-injector (model miniJet, USA).

Scanning Electron Microscopy (SEM)

SEM was performed with a Phillips microscope (model XL30, Guildford/England) operating at 20 kV. The samples were prepared by material deposition in an aluminum stub and gold-metalized.

Impedance Spectroscopy

Impedance measurements were obtained with films cut and sandwiched between two stainless steel electrodes assembled into an epoxy resin holder, as described previously.[22] The film thicknesses were 50 and 70 μm, and the area was about 1.5 cm^2. These films were obtained from samples prepared in a Carver press at 160°C and 5 ton/cm for 3 min. The measurements were performed with an (AUTOLAB PGSTAT 30/FRA 2, Metrohm-Netherlands) in the 1 MHz to 100 mHz frequency range, and the amplitude of the sinusoidal voltage was 10 mV. All experiments were carried out at 25°C.

Dynamic Mechanical Analysis (DMA)

Dynamic mechanical results were obtained with a DMA analyzer (TA Instruments model Q800). The specimens were analyzed in single-cantilever mode at a frequency of 1 Hz and a strain level of 0.1% in the temperature range of −140 to 120°C. The heating rate was 3°C/min. Testing was performed with rectangular bars with dimensions of approximately 17 × 13 × 3 mm^3. These were prepared with a Haake mini-injector (model miniJet). The injection was done at 165°C with a pressure of 250 bar for 4 s. The exact dimensions of each sample were measured before the scan.

RESULTS AND DISCUSSION

In a previous work,[21] we showed the synthesis and characterization of the nanocomposites examined in this study. The nanometric dimensions of the GNSs were demonstrated by TEM, XRD, and AFM. The TEM (Figure 1) and XRD results of the nanocomposites show the presence of intercalated and exfoliated graphite in the PE matrix.

Neat PE and the nanocomposites presented similar weight-average molecular weights of around 55,000 g/mol and a molecular weight distribution of around 3.0.

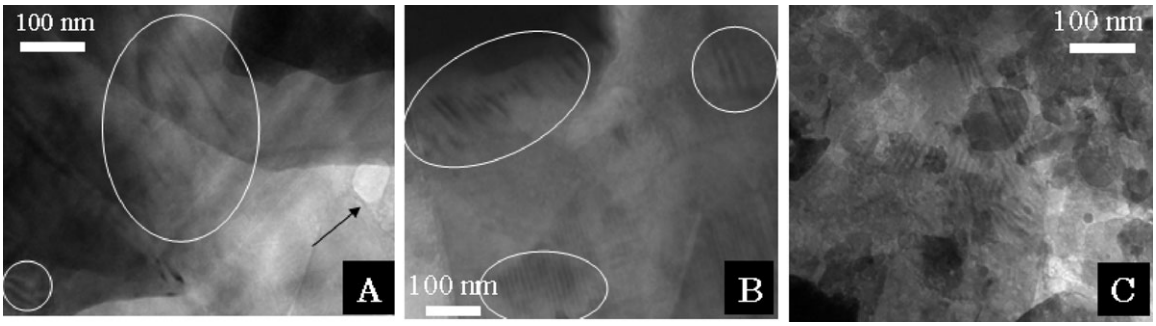

Figure 1. TEM micrographics of the nanocomposites: (a, b) PE/6.6% GNS and (c) PE/5.4% GNS.[19]

The thermal, mechanical, dynamic mechanical, and electrical properties are discussed in this article. Furthermore, in this study, we added to the nanocomposites 12.2, 15.3, and 20.9 wt % GNSs to determine the effect of a higher amount of GNSs on properties, such as the thermal and electrical properties.

Thermal Stability

The thermal stability of the PE–GNS nanocomposites was investigated by TGA. The thermogravimetric data are presented in Figure 2. This figure shows the TGA traces for the neat PE and the PE–GNS nanocomposites. It can be seen that the GNSs influenced the degradation temperature of the PE matrix by displacement of the curves to higher temperatures when compared with neat PE.

Table I shows the results obtained from the TGA curves. The onset degradation temperature increased around 30°C at 5.4 and 6.6 wt % of the GNS content in the nanocomposites compared to neat PE. The thermostability of the nanocomposites given by the maximum degradation temperature also increased by around 30°C for the nanocomposite with 15.3 wt % GNSs.

The degradation of HDPE produces mostly α-olefins such as propene and 1-hexene. This process occurs through a mechanism of cleavage of the polymeric chains.[23] Furthermore, this degradation becomes less effective when the polymeric chains decrease their mobility. The presence of graphene, which is a highly stable material and is stiffer than PE, confers rigidity to the polymeric matrix, decreasing the chain mobility and consequently retarding the degradation of the polymer.

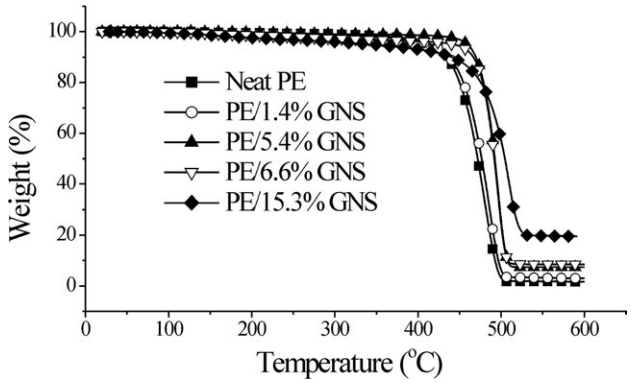

Figure 2. TGA curves of the neat PE and nanocomposites.

The fact that PE increased in stability in the presence of graphene suggested that the GNSs were well dispersed in the polymeric matrix. In addition to the dispersion of the filler, its concentration also had an important role in the thermal properties of the nanocomposites.[24]

Dynamic Mechanical Properties

All polymeric materials present viscoelastic behavior; in other words, when deformed, they simultaneously show the characteristics of plastic and elastic materials. DMA provides information about the viscoelastic behavior of the system, dismembering the module into two components: the elastic and viscous contribution.[25] The dynamic mechanical parameters of polymeric materials, such as the storage modulus (E'), loss modulus (E''), and mechanical damping (tan δ), are measured through the relaxation detection process. These relaxation processes correspond to transitions in which molecular rearrangements occur in the polymer chain. Normally, PE presents three main transitions. These transitions are called α, β, and γ in order of decreasing temperature. The γ relaxation generally occurs between -110 and -150°C. This relaxation corresponds to the glass transition and is related to the amorphous phase of the PE matrix. The β relaxation is seen only in LDPE around 0°C and refers to the relaxation of chain segments and side groups in the amorphous phase. HDPE does not present this peak because there are no branches in its polymer chains. The last relaxation, α, shows a peak between 50 and 120°C and is associated with the motion of chain segments in the crystalline phase.[26,27] The dependence of the dynamic mechanical properties on the temperature for the neat PE and nanocomposites is presented in Figures 3–5.

Figure 3 shows the variation of E' with temperature for the neat PE and the nanocomposites. It can be seen that all of the

Table I. Thermal Properties of the Neat PE and the Nanocomposites

Sample	T_{onset} (°C)	T_{max} (°C)
Neat PE	442 ± 1	480 ± 2
PE/1.4% GNS	454 ± 1	487 ± 1
PE/5.4% GNS	471 ± 1	494 ± 2
PE/6.6% GNS	472 ± 1	495 ± 1
PE/15.3% GNS	463 ± 1	510 ± 1

T_{onset}, initial degradation temperature.
T_{max}, maximum degradation temperature.

Applied Polymer SCIENCE

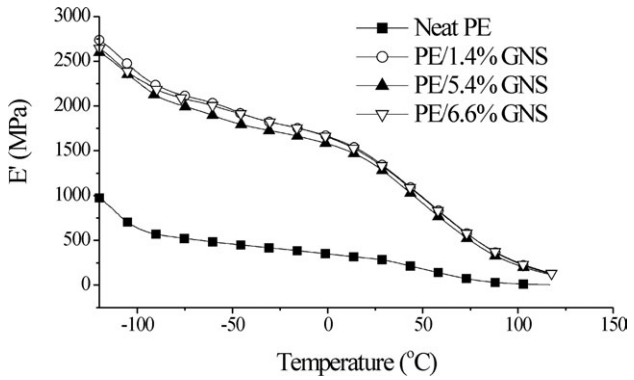

Figure 3. Variation of E' for the neat PE and the nanocomposites with temperature.

nanocomposites exhibited higher E' values than the neat PE. Already among the nanocomposites, there were no significant differences in the values of E'. As E' is similar to the elastic modulus or stiffness, this result indicates that the filler (GNSs) had a reinforcing effect on the polymer matrix, mainly in the region of the glass transition (the increase was 330% at −120°C). Furthermore, the value of E' remained higher for nanocomposites until around 120°C, when the curves began to move toward the baseline. This higher E' was the result of the large difference between the mechanical properties presented by the filler and the polymeric matrix. In fact, when PE changed from the glassy to the rubber state, the filler remained rigid in the entire temperature range; that is, the transitions that occurred were due to the polymeric matrix.[28]

E'' (Figure 4) is related to the viscous response of viscoelastic materials, and it reflects the amount of mechanical energy dissipated by the material.[29,30]

The curves in Figure 4 show the two transitions that HDPE presented, γ and α transitions. The higher value of E'' in the nanocomposites (in the two transitions) indicated a restriction in the mobility of the polymeric chain[29] as consequence of the addition of graphene to the polymeric matrix. This restriction could have been due to the confinement effect of two dimensional graphene nanosheets (2D–GNSs).[31] This resulted in a stiffer PE.

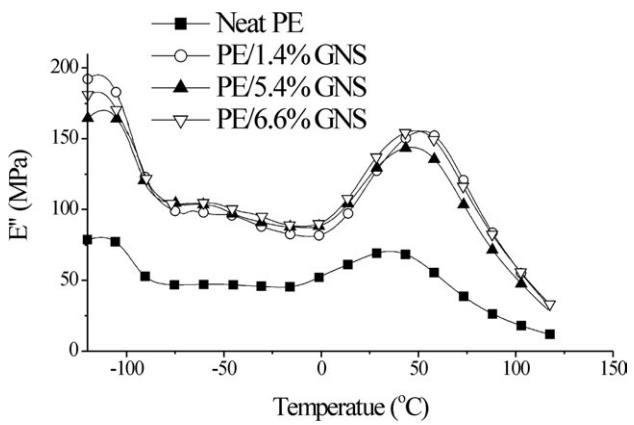

Figure 4. Variation of E'' with temperature for the neat PE and the nanocomposites.

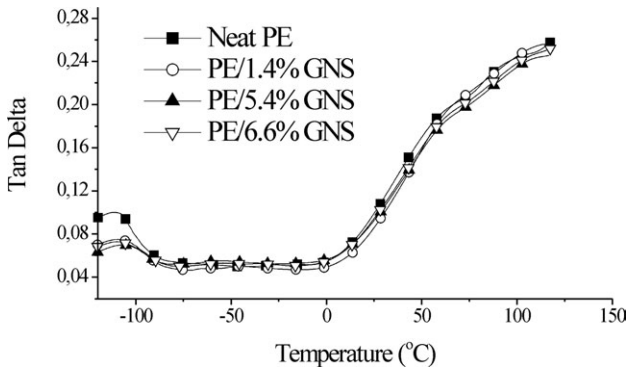

Figure 5. Variation of tan δ with temperature for the neat PE and the nanocomposites.

Mechanical damping gives the ratio between E'' (viscous contribution) and E' (elastic contribution). It indicates how distant the viscoelastic behavior of a material is from the neatly elastic behavior. A material with high damping dissipates much of the energy that was used to deform it. If the material is neatly viscous, it has an infinite damping; in other words, it has a total dissipation of the energy. On the other hand, if the material is neatly elastic, it does not present damping. The polymer materials are viscoelastic, so they have an intermediate behavior in relation to the dissipation of energy.[32]

According to Figure 5 and Table II, the nanocomposites showed lower tan δ values than the neat PE in the glass-transition temperature (T_g); this indicated that the viscoelastic energy dissipated less in the nanocomposites than in the neat polymer in the glass-transition region. Furthermore, low tan δ values were also attributed to good interactions between the filler and polymer.[33] The decrease in the peak height of the tan δ value of the nanocomposites showed that there was a strong interfacial interaction between graphene and polymeric matrix.[34] The fact that a major difference between the neat PE and the nanocomposites was in the γ-transition region suggested that the nanofiller was located mainly in the amorphous phase.

T_g was calculated from the tan δ curve. As shown in Table II, there was a small increase in the value of T_g in the nanocomposites with 5.4 wt % GNSs. The T_g peak shift to higher values indicated a constrained mobility of the chains of the polymeric matrix.[27] This was another indication of the reinforcement effect that the graphene sheets provided to PE.

Mechanical Properties

The mechanical properties of the nanocomposites prepared by *in situ* polymerization were investigated and are shown in Figures 6 and 7.

Table II. Variation of T_g for the Neat PE and the Nanocomposites

Sample	T_g (°C)	Tan δ
Neat PE	−111	0.100
PE/1.4% GNS	−109	0.075
PE/5.4% GNS	−106	0.070
PE/6.6% GNS	−109	0.073

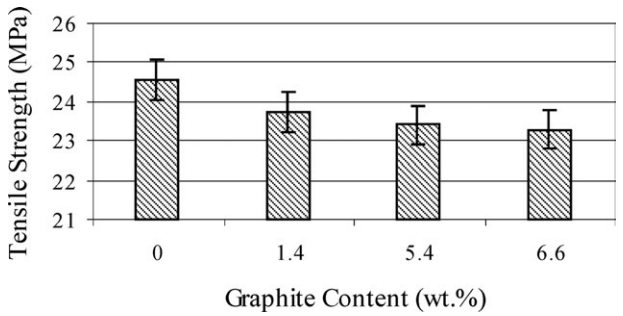

Figure 6. Effects of GNS on the tensile strength for the nanocomposites.

Figure 6 shows a slight decrease (<5%) in the tensile strength of the nanocomposites in relation to the neat PE. Chen et al.[35] also observed a reduction in the tensile strength in HDPE–expanded graphite nanocomposites and attributed this behavior to a reduction in the mobility of the HDPE molecules, which made the molecules unable to dissipate the mechanical energy applied.

It is shown in Figure 7 that the elastic modulus remained constant with the addition of 1.4 wt % GNSs and increased with higher graphite contents. The elongation at break decreased and reached a limit at the GNS content of 6.6 wt %. The increase in the elastic modulus (Figure 7) showed that the material became stiffer. To understand the decrease of the elongation at break, the morphology of the fracture surfaces was studied.

Morphology of the Fracture Surfaces

SEM analysis was used to investigate the kind of fracture that the graphene sheets caused in the PE matrix after the samples passed through the tensile tests. Figure 8 shows the fractured sections of the neat PE and the nanocomposites. From Figure 8(A, B), it can be seen that the neat PE broke with a fibrous morphology and that the addition of 1.4 wt % graphene in the matrix was not sufficient to change this morphology. These images show that the PE broke with long fibrils and showed crazing or deformation zones.[36] Therefore, a ductile fracture occurred in the neat PE and in the 1.4 wt % GNS nanocomposite. However, when a larger amount of GNS was added [Figure 8(C, D)], the fracture became brittle. On the other hand, increased magnification [Figure 8(E, F)] showed a subtle difference between the nanocomposites with 5.4 and 6.6 wt % GNSs. In fact, in the fracture section of the nanocomposite with 5.4 wt % GNSs, the presence of more short fibers of PE could be seen than in the 6.6 wt % one. This showed clearly that the GNSs dispersed in the polymeric matrix and inhibited the formation of a PE fiber morphology.

The morphology of the fracture surfaces study showed that the presence of GNSs decreased the ductility of PE and produced an embrittlement effect.

Impedance Spectroscopy Measurements

The PE–GNS nanocomposites were investigated with the electrochemical impedance spectroscopy technique to determine the polymer conductivity.[37] The impedance is represented by a complex plane composed of real and imaginary parts. The real part represents the bulk resistance (R_b), and the imaginary part represents the reactance arising from the capacitive or inductive nature of the system.[38] R_b can be determined from the study of the variation of the impedance with frequency. The electrical conductivity of the polymeric film can be calculated by the following equation:

$$\sigma = 1/R_b(d/S)$$

where σ is the electrical conductivity, d is the film thickness, and S is the area of electrodes contacting the polymeric film. The electrical conductivity of the PE–GNS nanocomposites was determined from the R_b values, which were obtained by the fitting of the experimental diagrams (not given here) with the FRA system software.

Table III presents the electrical conductivity values and the corresponding GNS values in weight and volume percentage for the nanocomposites.

The neat PE presented an electrical conductivity of 1.4×10^{-13} S/cm, which remained practically unchanged with the addition of 0.52 vol % graphite (2.4×10^{-13} S/cm). An enhancement of the electrical conductivity by over 10,000 times was detected with the addition of 5.2 vol % graphene, with the conductivity reaching around 6.6×10^{-8} S/cm. Thus, with increasing content of GNSs up to 8.9 vol % in PE, the mobility of the network and the density of the potential charge carriers were also

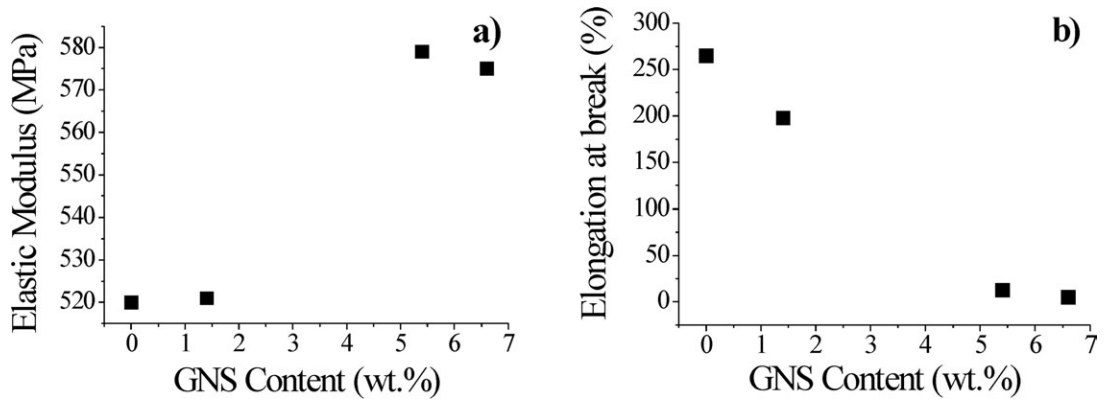

Figure 7. Dependence of the neat PE and the nanocomposites on the graphene content: (a) elastic modulus and (b) elongation at break.

Applied Polymer SCIENCE

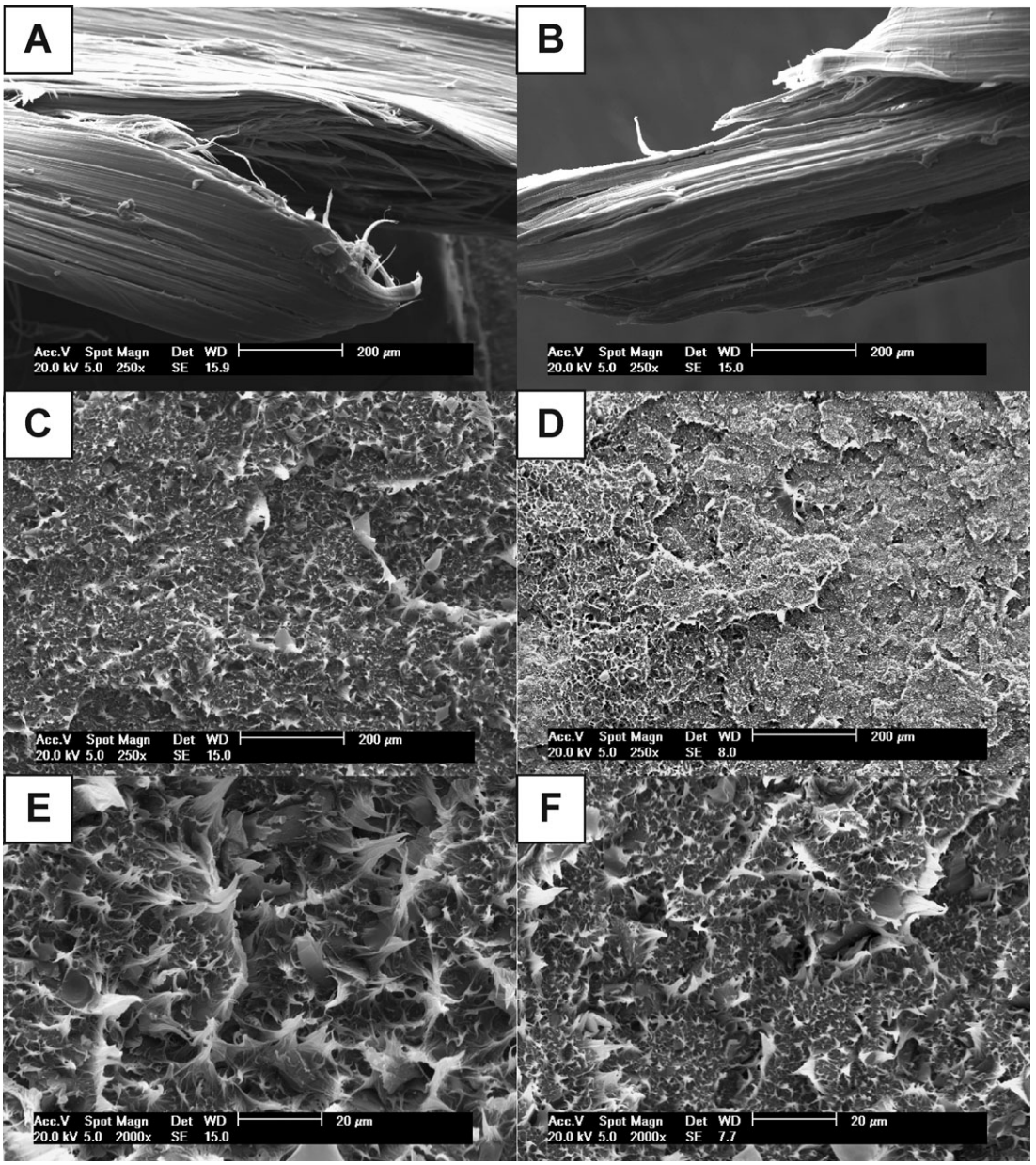

Figure 8. SEM images of the broken tensile sections at the same magnification for (A) neat PE, (B) PE/1.4% GNS, (C) PE/5.4% GNS, and (D) PE/6.6% GNS and at greater magnification for (E) PE/5.4% GNS and (F) PE/6.6% GNS.

increased, and this influenced the electrical conductivity, as shown in Figure 9.

The marked gap in the conductivity in Figure 9 corresponds to the percolation threshold. Percolation theory is based on the development of a conductive network formed by electron transport paths through the volume of the sample.[38] The electrical properties of polymer nanocomposites are strongly dependent on the distribution of the conductor filler in the polymer matrix. It is fundamental that filler particles contact each other to form conductive networks because these particles are dispersed on an insulating polymer matrix. The graphite could contact the PE matrix plane to plane, edge to edge (cross or parallel), and edge to plane. The most effective way of having electrical

Table III. Nanocomposite Electrical Conductivity and Corresponding Values of the GNSs (vol % and wt %)

GNS wt %	GNS vol %	σ (S/cm)
0	0	1.4×10^{-13}
1.4	0.5	2.4×10^{-13}
5.4	1.2	3.9×10^{-13}
6.6	2.4	5.5×10^{-12}
12.2	5.2	6.6×10^{-8}
14.3	6.1	1.6×10^{-7}
15.3	6.6	2.4×10^{-7}
20.9	8.9	1.3×10^{-4}

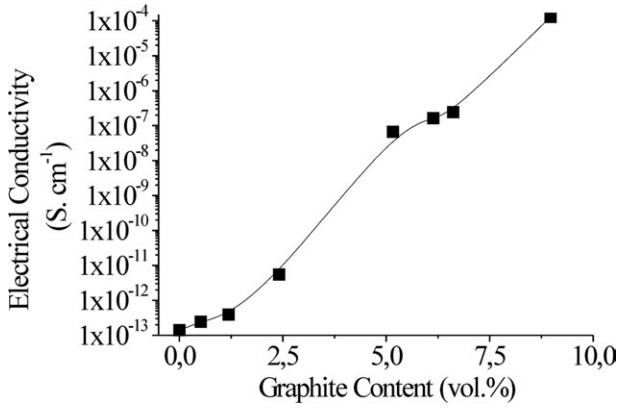

Figure 9. Dependence of the electrical conductivity on the GNS variation.

conductivity in an insulating matrix, such as PE, is when graphite is dispersed plane to plane in the matrix. Therefore, the orientation of the conductor filler plays an important role in the electrical conductivity of the material. In the *in situ* polymerization method, graphite can be dispersed in both ways.

Percolation thresholds are achieved with a very low amount of graphite by melt mixing when graphite was not homogeneously dispersed in the polymeric matrix. It seems that a slight aggregation of the conductor filler may improve the maximum electrical conductivity.[14] According Panwar and Mehra,[39] infinite cluster sites interconnected for filler concentration higher than a certain threshold value have played an important role in the low percolation threshold. They prepared PE–graphite composites by hot compression molding, and the critical percolation threshold was obtained with a filler loading of about 5 wt %.

On the other hand, Li and Chen[24] made PE–expanded graphite nanocomposites by a master-batch filling method, and they obtained a percolation threshold of about 16 wt %. When they prepared the nanocomposites by a direct melt extrusion process, an even higher value of the critical percolation threshold was obtained, about 20 wt %. In a recent work,[40] HDPE–graphite nanocomposites were prepared by melt mixing to investigate the effect of graphite on the electrical properties of the HDPE matrix. The authors estimated that the percolation threshold was between 15 and 20 vol % graphite.

The critical percolation threshold of a nanocomposite can be determined from the classical equations of percolation theory. According to the percolation theory, the conductivity (σ) of the nanocomposite can be calculated by the following equation:

$$\sigma = \sigma_0(\varphi - \varphi_c)^t$$

where φ is the volume fraction of the fillers, φ_c is the percolation volume fraction, and σ and σ_0 are the conductivity of the composite and proportionality constants, respectively, which are related to the intrinsic conductivity of the filler. The critical exponent (t) reflects the system dimensionality of the nanocomposite, and it follows a power law dependence of approximately 1–1.3 in a two-dimensional system.[41]

In this article, we used the SPSS statistical program (Federal University of Rio Grande do Sul/Brazil) to measure the critical percolation threshold, and the results after fitting revealed a value of the critical exponent of 1.03.

The PE–GNS nanocomposites synthesized in this study by an *in situ* polymerization method showed a critical percolation threshold of about 3.8 vol % GNSs; this corresponded to 8.4 wt % GNSs and was much lower than that obtained by the master-batch or melt extrusion methods. However, our percolation threshold was quite high compared with that obtained by hot compression molding. This result could be explained by the good dispersion of nanoparticles obtained by *in situ* polymerization, in which the PE grew around the filler, isolating the GNSs with a layer of insulating material. This was unfavorable for the creation of a path for the transport of electrons and, hence, for the electrical network.

CONCLUSIONS

A study of the properties of PE–GNSs obtained by *in situ* polymerization was performed. A substantial improvement in the thermal stability of the nanocomposites was observed in the presence of graphene sheets. The onset degradation temperature increased by 30°C in the nanocomposites with 1.4 and 5.4 wt % GNSs, and the nanocomposite with 15.3 wt % GNSs presented an increase of 30°C in the maximum degradation temperature in relation to that of neat PE.

The higher values in E' and E'' of the nanocomposites compared to neat PE showed that the GNSs provided a reinforcing effect on the PE matrix. The nanocomposites showed a slight decrease in the tensile strength (ca. 5% for PE/6.6 wt % GNSs) in relation to the neat polymer. Furthermore, the increase in the elastic modulus, the decrease in the elongation at break, and the shift of the T_g peak to higher values indicated that the polymer became stiffer.

The PE–GNS nanocomposites presented a critical percolation threshold of about 3.8 vol % (8.4 wt %) GNSs; above this amount of GNSs, the insulating material became a semiconductor.

ACKNOWLEDGMENTS

The authors thank Coordenação de Aperfeiçoamento de Pessoal de Nível Superior (CAPES) and Conselho Nacional de Desenvolvimento Científico e Tecnológico (CNPQ) for financial support of this research project and Nacional de Grafite Ltda. for supplying the graphite Micrograf HC11.

REFERENCES

1. Chrissafis, K.; Paraskevopoulos, K. M.; Tsiaoussis, I.; Bikiaris, D. *J. Appl. Polym. Sci.* **2009,** *114*, 1606.
2. Kaminsky, W.; Funck, A. *Macromol. Symp.* **2007,** *260*, 1.
3. Keledi, G.; Hári, J.; Pukánszky, B. *Nanoscale* **2012,** *4*, 1919.
4. Ophir, A.; Dotan, A.; Belinsky, I.; Kenig, S. *J. Appl. Polym. Sci.* **2010,** *116*, 72.
5. Zapata, P.; Quijada, R.; Retuert, J.; Moncada, E. *J. Appl. Polym. Sci.* **2009,** *113*, 2368.

6. Li, S.; Chen, H.; Cui, D.; Li, J.; Zhang, Z.; Wang, Y.; Tang, T. *Polym. Compos.* **2010,** *31*, 504.
7. Wood, W.; Li, B.; Zhong, W. H. *Polym. Eng. Sci.* **2010,** *50*, 613.
8. Parvinzadeh, M.; Moradian, S.; Rachidi, A.; Yazdanchenas, M. E. *Appl. Surf. Sci.* **2010,** *256*, 2792.
9. Pluta, M.; Alexandre, M.; Blacher, S.; Dubois, P.; Jerome, R. *Polymer* **2001,** *42*, 9293.
10. Kim, H.; Abdala, A. A.; Macosko, C. W. *Macromolecules* **2010,** *43*, 6515.
11. Wakabayashi, K.; Pierre, C.; Dikin, D. A.; Ruoff, R. S.; Ramanathan, T.; Brinson, L. C.; Torkelson, J. M. *Macromolecules* **2008,** *41*, 1905.
12. (a) Du, J.; Zhao, L.; Zeng, Y.; Zhang, L.; Li, F.; Liu, P. *Carbon* **2011,** *49*, 1094; (b) Bredeu, S.; Peeterbroeck, S.; Bonduel, D.; Alexandre, M.; Dubois, P. *Polym. Int.* **2008,** *57*, 547.
13. Zheng, W.; Lu, X.; Wong, S.-C. *J. Appl. Polym. Sci.* **2004,** *91*, 2781.
14. Potts, J. R.; Dreyer, D. R.; Bielawski, C. W.; Ruoff, R. S. *Polymer* **2011,** *52*, 5.
15. Kalaitzidou, K.; Fukushima, H.; Drzal, L. T. *Compos. Sci. Technol.* **2007,** *67*, 2045.
16. Wang, L.; Chen G. *J. Appl. Polym. Sci.* **2010,** *116*, 2029.
17. Wang, J.; Xu, C.; Hu, H.; Wan, L.; Chen, R.; Zheng, H.; Liu, F.; Zhang, M.; Shang, X.; Wang, X. *J. Nanopart. Res.* **2011,** *13*, 869.
18. Kim, H.; Kobayashi, S.; AbdurRahim, M. A.; Zhang, M. J.; Khusainova, A.; Hillmyer, M. A.; Abdala, A. A.; Macosko, C. W. *Polymer* **2011,** *52*, 1837.
19. (a)Jiang, X.; Drzal, L. T. *J. Appl. Polym. Sci.* **2012,** *124*, 525; (b)*Polym. Compos.* **2012,** *33*, 636.
20. Pang, H.; Chen, T.; Zhang, G.; Zeng, B.; Li, Z.-M. *Mater. Lett.* **2010,** *64*, 2226.
21. Fim, de, C. F.; Guterres, J. M.; Basso, N. R. S.; Galland, G. B. *J. Polym. Sci. Part A: Polym. Chem.* **2010,** *48*, 692.
22. Rodrigues, I. R.; Forte, M. M. C.; Azambuja, D. S.; Castagno, K. R. L. *React. Funct. Polym.* **2007,** *67*, 708.
23. Lucas, E. F.; Soares, B. G.; Monteiro, E. E. C. In Caracterização de Polímeros: Determinação de Peso Molecular e Análise Térmica. Rio de Janeiro E-Papers, **2001.**
24. Li, Y. C.; Chen, G. H. *Polym. Eng. Sci.* **2007,** *47*, 882.
25. Lozano, K.; Barrera, E. V. *J. Appl. Polym. Sci.* **2001,** *79*, 125.
26. Yang, S.; Taha-Tijerina, J.; Serrato-Diaz, V.; Hernandez, K.; Lozano, K. *Compos. B* **2007,** *38*, 228.
27. Pegoretti, A.; Ashkar, M.; Migliaresi, C.; Marom, G. *Compos. Sci. Technol.* **2000,** *60*, 1181.
28. Baniasadi, H.; Ramazani, A.; Javan Nikkhah, S. *Mater. Des.* **2010,** *31*, 76.
29. Jayanarayanan, K.; Thomas, S.; Joseph, K. *Compos. A* **2008,** *39*, 164.
30. Vasiljevic-Shikaleska, A.; Popovska-Pavlovska, F.; Cimmino, S.; Duraccio, D.; Silvestre, C. *J. Appl. Polym. Sci.* **2010,** *118*, 1320.
31. Pramoda, K. P.; Hussain, H.; Koh, H. M.; Tan, H. R.; He, C. B. *J. Polym. Sci Part A: Polym. Chem.* **2010,** *48*, 4262.
32. Canevarolo, S. V. J. In Técnicas de Caracterização de Polímeros; Artliber: São Paulo, Brazil, **2004.**
33. Kar, S.; Maji, P. K.; Bhowmick, A. K. *J. Mater. Sci.* **2010,** *45*, 64.
34. Barick, A. K.; Tripathy, D. K. *Polym. Eng. Sci.* **2010,** *50*, 484.
35. She, Y.; Chen, G.; Wu, D. *Polym. Int.* **2007,** *56*, 679.
36. Sui, G.; Zhong, W. H.; Ren, X.; Wang, X. Q.; Yang, X. P. *Mat. Chem. Phys.* **2009,** *115*, 404.
37. Wang, M.; Zhao, F.; Guo, Z.; Dong, S. *Electrochim. Acta* **2004,** *49*, 3595.
38. Nanda, M.; Tripathy, D. K. *J. Appl. Polym. Sci.* **2010,** *116*, 2758.
39. Panwar, V.; Mehra, R. M. *Polym. Eng. Sci.* **2008,** *48*, 2178.
40. Tavman, I.; Krupa, I.; Omastova, M.; Sarikanat, M.; Novak, I.; Sever, K.; Ozdemir, I.; Seki, Y.; Podhradská, S.; Moskova, D.; Erbay, E.; Guner, F. *Polym. Compos.* **2012,** *33*, 1071.
41. Gao, J.-F.; Li, Z.-M.; Meng, Q.; Yang, Q. *Mater. Lett.* **2008,** *62*, 3530.